An Experimental Investigation on the Effect of Exhaust Gas Recirculation in a Small-Scale Fixed Bed Biomass Boiler

Gianluca Caposciutti[a], Marco Antonelli[a], Federica Barontini[b,*], Chiara Galletti[b], Leonardo Tognotti[b], Umberto Desideri[a]

[a] Dipartimento di Ingegneria dell'Energia, dei Sistemi, del Territorio e delle Costruzioni, Università di Pisa, Largo Lucio Lazzarino 2, 56122 Pisa, Italy
[b] Dipartimento di Ingegneria Civile e Industriale, Università di Pisa, Largo Lucio Lazzarino 2, 56122 Pisa, Italy
 federica.barontini@unipi.it

Exhaust gas recirculation is a technique that allows for controlling the combustion chamber temperature and reducing the NO_x and particle matter emissions. Moreover, it helps to mitigate soot formation and ash agglomeration in combustion systems. The present study investigated the effect of exhaust gas recirculation on combustion temperatures of a 140 kW underfed stoker biomass boiler. To this purpose, a wide range of operating conditions were used, collecting data regarding flue gas and fixed bed temperatures. It turned out that the recirculating ratio has a significant effect on the temperatures in the primary combustion zone, affecting the thermal gradient and the main thermal zones of the biomass combusting bed. The obtained results can be useful for lumped parameter modeling, or CFD validation purposes.

1. Introduction

With the increment in the world energy demand and the increasing concerns on environmental pollution, global warming, and climate change, the use of renewable, sustainable, and environmentally-friendly energy resources has become mandatory. In this scenario, biomass appears as one of the most promising renewable energy resources, because of its abundance, wide distribution, and carbon dioxide neutrality. Among all biomass-to-energy conversion technologies, biomass combustion for heat and power generation represents the most common and efficient conversion route. Stoves and boilers fed with biomass woodchips have a wide broad market share in Europe, especially for small-power applications. However, further efforts in the design and operation of these devices are still required to improve their performance in terms of efficiency and pollutant emissions. In particular, the NO_x, CO and particulate matter emissions pose a growing concern for the recent European regulations in terms of air quality. Therefore, several strategies have been proposed to reduce pollutant emissions from such devices, such as air staging and exhaust gas recirculation. Amongst them, exhaust gas recirculation (EGR) can provide key advantages. Firstly, relative air-fuel velocity and combustion turbulence can be increased without increasing the oxygen excess in the combustion chamber. Secondly, the fuel bed temperature can be limited thanks to the reduced oxygen availability, thus reducing NO_x production, also mitigating ash agglomeration and soot transport phenomena.

However, the potential of the EGR technique has been scarcely explored in the literature. Schulte et al. (2020) proved that the use of EGR in combination with a low excess air ratio in the fuel bed, could reduce particulate matter emissions from a pellet boiler. Archan et al. (2021) developed and experimentally investigated a small-scale (200 kW) multi-fuel biomass grate furnace, employing a low oxygen concentration in the bed and a double air staging, including the supply of flue gas recirculation. Their results indicate a positive influence of recirculated flue gas on NO_x emissions, since the EGR utilization within the reduction zone limits the NO_x formation potential by minimizing local temperature peaks and lowering the oxygen partial pressure. Numerical models, specifically Computational Fluid Dynamics (CFD) models, were applied to the theoretical study of the effect of EGR on boiler performance and gas contaminant emissions. Gomez et al. (2019) carried out several simulations of a 30 kW boiler operating in different conditions: the results showed that EGR can increase the boiler thermal

performance and reduce the NO_x emissions, especially for low oxygen excess values. The results of the CFD modelling study of a 13 MW waste wood-fired grate boiler performed by Rajh et al. (2018) indicated that an optimized configuration of the air and recycled flue gas jets can greatly enhance mixing and extend the residence time of the combustibles in the hot zones in the furnace, and therefore improve combustion and reduce pollutant emissions, especially those due to incomplete combustion such as CO. The availability of specific experimental data is crucial for the development and validation of numerical models, that could be used to improve the performance of biomass boilers (Patronelli et al., 2018).

In the present work, the effect of the EGR was experimentally studied in a 140 kW fixed-bed biomass boiler. To this purpose, the boiler was equipped with control and measuring systems to analyze temperature, mass flow and gas composition. More specifically, the temperatures in the fuel bed and the exhaust gas composition were monitored under different operating conditions, i.e., equivalence ratio, primary to secondary air-flow ratio, and EGR ratio, to assess the potential of EGR in biomass furnaces.

2. Method

The fixed bed boiler is a 140 kW underfed stocker belonging to the University of Pisa and is shown in Figure 1a. The fixed bed has a 600 mm length, 150 mm width, and 200 mm depth, and it is equipped with a screw feeder (having an 80 mm diameter and 80 mm step) providing the biomass flow m_B at a constant rate from below the bed (see Figure 1b). The total air flow is supplied by a 2.2 kW centrifugal blower, and it is split into primary and secondary flows using two sphere-valves. The primary air is injected 20 mm below the biomass fixed bed surface through 68 rectangular nozzles (20 mm length and 3 mm height), distributed in 3 rows around the fixed bed. The secondary air is fed around the biomass bed through a stainless-steel pipe system and injected by 7 circular ducts (20 mm diameter). An exhaust gas blower extracts the flue gases from the combustion chamber and to keep the pressure at 20 Pa below the ambient one for safety reasons. After the combustion stage, a gas-to-oil heat exchanger heats up a Seriola 1510 diathermic oil, thus transferring the heat to a Kettle water boiler.

More details about the boiler are given in previous works (Caposciutti et al., 2018, 2020); however, with respect to these works the boiler was modified here to recirculate the exhaust gases. More specifically, the exhaust gases are extracted downstream of the heat exchanger, with a m_R mass flow rate, and subsequently are mixed with the primary air. The value of m_R is controlled by means of a 0.75 kW high-temperature blower and a gate valve, while m_R is evaluated through a stagnation pressure measurement system.

The primary and secondary air mass flow rates, i.e., $m_{a,p}$ and $m_{a,s}$, respectively, are measured by using two TFLOW T112 hot wire sensors. The heat exchanger gas inlet and outlet temperatures (namely $T_{f,in}$ and $T_{f,out}$, respectively) are monitored by means of radiation-shielded k-type thermocouples. The flue gas composition, in terms of CO_2 and O_2, is monitored by means of a NDIR and a paramagnetic-based instruments from Environnement SA for mass balance calculation. A scheme of the measuring system is provided in Figure 2a.

The fixed bed is instrumented with 12 k-type thermocouples to measure the temperature in several positions, as described by the scheme in Figure 2b. These are mounted on a stainless-steel housing to keep them in position during the operation. The thermal sensor housing is designed to limit the interaction with the biomass and gas flow.

(a)

(b)
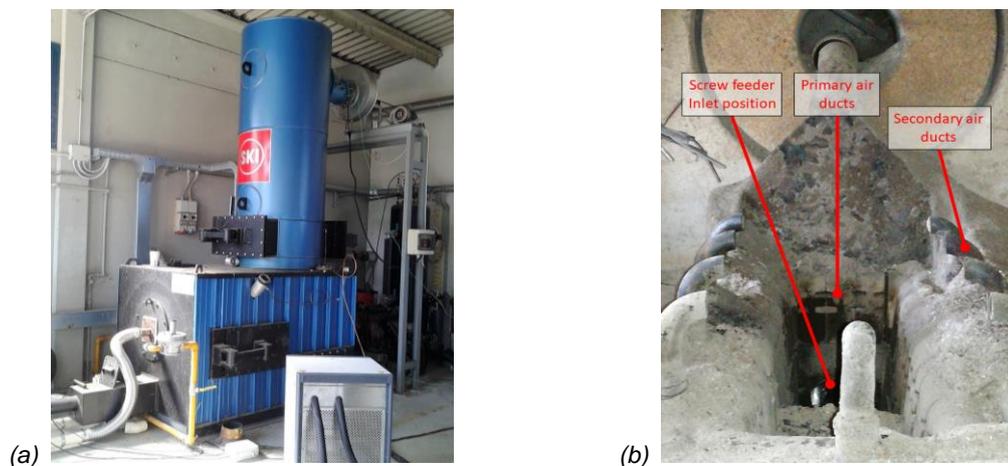
Figure 1: Picture of the boiler (a) and fixed bed (b).

(a)

(b)
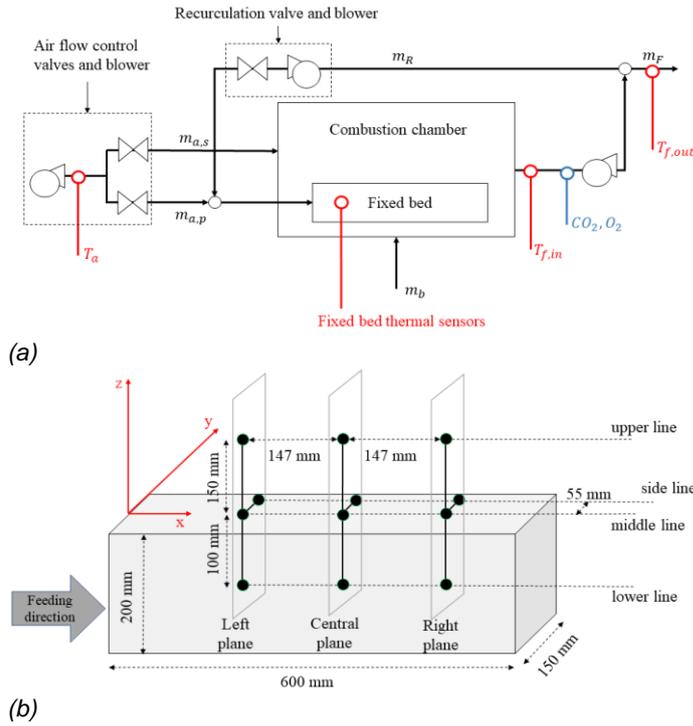
Figure 2. Scheme of the system (a) and of thermocouples displacement (i.e., black dots) in the fixed bed (b).

For the thermocouple displacement, three *ZY* planes were considered with different distances from the biomass flow inlet, thus the Left, Central, and Right planes were chosen. The distance of the Left plane from the biomass inlet was 315 mm. Three lines on the *ZX* fixed bed symmetry plane were chosen to be 100 mm below the biomass surface (i.e., lower line), on the biomass surface (i.e., middle line), and 150 mm above it (i.e., upper line), the latter corresponding to the secondary air inlet position. Finally, a side-line was defined on the biomass surface, i.e., in the *XY* plane, at a distance of 55 mm from the middle line.

Hence, the fixed bed thermal behavior was reconstructed by using linear interpolation of the temperatures measured in the positions shown in Figure 2b, allowing to evaluate this behaviour for different operating conditions.

The air excess ratio is

$$\lambda = \frac{\alpha}{\alpha_{st}} \tag{1}$$

where α represents the air-to-fuel ratio

$$\alpha = \frac{m_{a,p} + m_{a,s}}{m_b} \tag{2}$$

In the present system, α can be directly derived from the flue gas oxygen content, and m_b is calculated from the air-to-fuel ratio knowing the total air flow rate (Caposciutti et al., 2018).

Moreover, the primary air excess ratio can be defined as :

$$\lambda_p = \frac{m_{a,p}}{m_b} \frac{1}{\alpha_{st}} = \frac{\alpha_p}{\alpha_{st}} \tag{3}$$

Finally, the recirculation ratio *R* represents the ratio between the recirculated and total flue gas mass flow, i.e.:

$$R = \frac{m_R}{m_F} \tag{4}$$

The biomass was poplar woodchips whose composition is reported in Table 1.

Table 1: Biomass characteristics.

C	H	N	O	Moisture	Ash	LHV
(%daf)	(%daf)	(%daf)	(%daf)	(%ar)	(%db)	(MJ/kg)
48.76	5.68	0.21	45.35	10.06	0.9	17.88

λ, λ_p, and R are the main operation parameters. Tests were performed by varying both λ and λ_p. To evaluate the effect of R, all the tests were repeated at the approximately same (λ, λ_p) conditions, while the gate valve was controlled to ensure R to be around 0, 0.3 and 0.6. Totally, 12 operating points were investigated. All the temperature and mass flow measurements were managed by means of a NI9214, and a NI9207 boards with a NI9223 chassis, and a Labview-based software. Data were sampled for at least 30 min in steady state condition.

3. Results and discussion

The resulting operating conditions and flue gas temperatures measured in the experimental tests are reported in Table 2, where the different IDs refer to different operating conditions. Consistently with the literature (Carroll et al., 2015; Lamberg et al., 2011), λ was varied between 1.1 and 3, while λ_p between 0.1 and 0.6. To assess the effect of R, the tests were replicated at the approximately same (λ, λ_p) conditions, with different R values, namely around 0, 0.3 and 0.6.

Table 2: Obtained operating conditions

	ID1	ID2	ID3	ID4	ID5	ID6	ID7	ID8	ID9	ID10	ID11	ID12
λ (-)	1.21	1.44	1.24	1.35	1.41	1.96	1.45	1.10	1.20	2.53	1.93	3.27
λ_p (-)	0.50	0.43	0.28	0.15	0.35	0.25	0.13	0.39	0.56	0.31	0.23	0.20
R (-)	0	0	0.46	0.55	0	0.40	0.48	0.57	0.76	0	0.34	0.30
$T_{f,in}$ (°C)	669	696	698	728	766	722	763	838	830	698	744	686

Figure 3 shows the average fuel bed temperature as a function of λ_p, and R. The average fuel bed temperature is obtained by averaging the 9 temperature measurements in the bed. It can be observed how such temperature increases with the recirculation ratio, which mixes a high temperature stream with the primary air feeding the bed. For low R values, results indicate a non-monotic trend of the average temperature with λ_p thus indicating the presence of an optimal value of such parameter to trigger combustion. For low λ_p and R, combustion is hampered by the low mixing and oxygen availability; further increasing λ_p the average temperature increases up to a maximum value. Subsequently, the average temperature decreases because of the dilution with primary air. With increasing R such behaviour is hampered by the increased mixing and turbulence in the reaction region which promote combustion and lead to high temperatures.
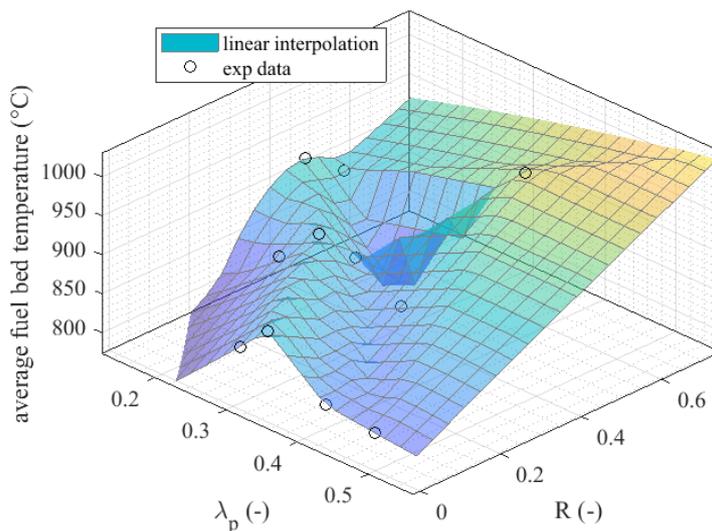
Figure 3. Average fuel bed temperature vs λ_p and R.

Figure 4 shows the temperatures in the biomass primary combustion area. The top panels refer to the vertical *ZX* plane, while the bottom panels to the horizontal *YX* plane (see Figure 2b). Six conditions in terms of λ, λ_p and *R* are selected, even though two pairs conditions match each other closely and are devised to assess the accuracy of the measurements.
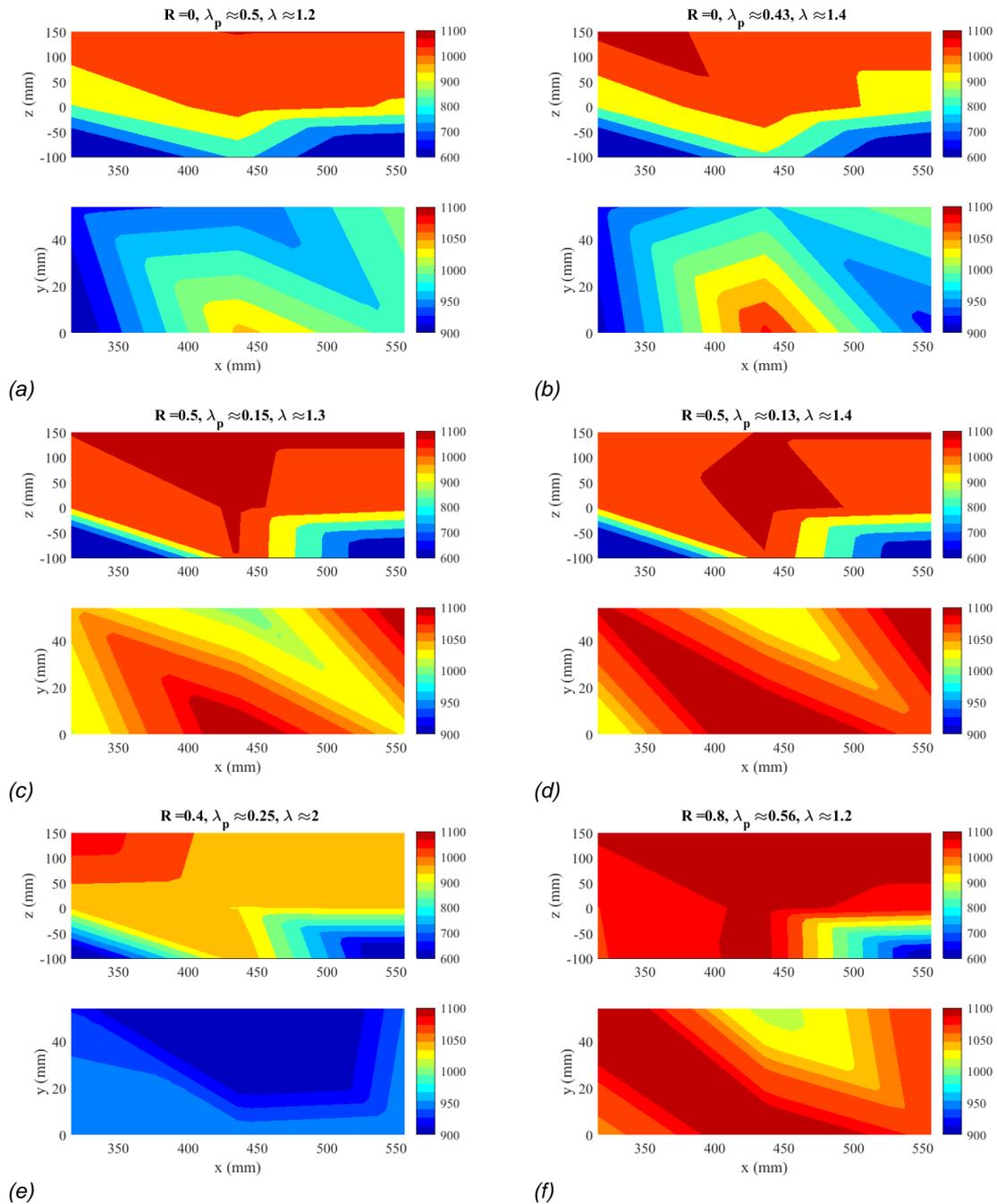
Figure 4. Temperature spatial distribution in the biomass primary combustion area: ZX (top panel) and YX (bottom panel) planes. a) ID1; b) ID2; c) ID4; d) ID7; e) ID6; f) ID9. See Table 2 for more details on operating conditions.

Indeed, Figure 4 shows good repeatability in temperature distributions obtained with similar operating conditions, as shown by comparing Figure 4a (ID1) with Figure 4b (ID2) and Figure 4c (ID4) with Figure 4d (ID7). The temperature distribution showed a larger disuniformity when no recirculation was used. When *R* was

increased, the temperature on the bed surface was more uniform and its average temperature reached its maximum. This fact was verified at constant air excess ratio, both by increasing R and lowering λ_p (Figure 4a-b against Figure 4c-d, i.e. ID1-ID2 against ID4-ID7), or by increasing R at constant λ_p (Figure 4a-b against Figure 4f, i.e. ID1-ID2 against ID9). On the other hand, increasing R had a negligible effect on the fuel bed temperatures for high air excess ratios, as also shown by Figure 3, because of a large amount of cold air injected into the system (see Figure 4e, i.e. ID6). Figure 4 shows that different thermal regions appear in the solid biomass zone from the left to the right area of the fixed bed.

On the bottom-left side of the fuel bed, lower temperatures were found possibly due to the high moisture content of the biomass; a drying phase near the inlet region appeared due to the fresh fuel supply. In the central area, the higher temperature indicated that combustion reactions, both in gas and solid phase, took place. In all the cases, the bottom-right side of the fuel bed temperatures were lower than 600 °C. This was due to the accumulation of depleted fuel promoted by the motion of the screw feeder, which pushed fresh biomass from the bottom-left to the bottom-right of the system. This fact was already observed in other recent studies involving the same device in different operating conditions (Caposciutti et al., 2018). Figure 4 also highlights that the EGR can drastically affect the extent of these zones. In particular, large gas recirculation pushed the drying zone towards the inlet position, resulting in a more uniform temperature profile in the remaining part of the fixed bed.

4. Conclusions

Exhaust gas recirculation was investigated in a 140 kW biomass underfed stoker boiler to analyse its impact on the temperatures in the combustion region. In particular, the temperature distribution inside and above the fixed bed was analyzed as a function of the air excess and recirculation ratios. When the recirculation was introduced, the behaviour of the average bed temperature versus the air excess ratio changed. Without recirculation, in facts, an optimal value of the air excess exists, as a result of the interplay between better mixing and fresh air dilution. When the recirculation was increased, this trend was smoothed and the average temperature trend with the excess ratio resulted more uniform. The recirculation ratio also affects the behaviour of the fixed bed local temperatures. For similar air excess ratios, a higher rate of recirculated flue gas increases the average biomass bed temperatures and leads to a more even temperature distribution. Moreover, it pushes the main reaction area towards the fuel inlet zone, drastically affecting the thermal zones distribution in the bed of combusting biomass. These details can be useful for developing solid combustion lumped-parameter models, and for validating CFD models. For instance, the present data may support the development of in-bed models based on reactor networks to be coupled to freeboard CFD calculations.

References

Archan G., Anca-Couce A., Buchmayr M., Hochenauer C., Gruber J., Scharler R., 2021, Experimental Evaluation of Primary Measures for NO_X and Dust Emission Reduction in a Novel 200 kW Multi-Fuel Biomass Boiler, Renewable Energy, 170, 1186–96.

Caposciutti G., Barontini F., Antonelli M., Tognotti L., Desideri U., 2018, Experimental Investigation on the Air Excess and Air Displacement Influence on Early Stage and Complete Combustion Gaseous Emissions of a Small Scale Fixed Bed Biomass Boiler, Applied Energy, 216, 576–87.

Caposciutti G., Barontini F., Galletti C., Antonelli M. Tognotti L., Desideri U., 2020, Woodchip Size Effect on Combustion Temperatures and Volatiles in a Small-Scale Fixed Bed Biomass Boiler, Renewable Energy, 151, 161-174.

Carroll J.P., Finnan J.M, Biedermann F., Brunner T., Obernberger I., 2015, Air Staging to Reduce Emissions from Energy Crop Combustion in Small Scale Applications, Fuel 155, 37–43.

Gómez M.A., Martín R., Chapela S., Porteiro J., 2019, Steady CFD Combustion Modeling for Biomass Boilers: An Application to the Study of the Exhaust Gas Recirculation Performance, Energy Conversion and Management, 179, 91–103.

Lamberg H., Sippula O., Tissari J., Jokiniemi J., 2011, Effects of Air Staging and Load on Fine-Particle and Gaseous Emissions from a Small-Scale Pellet Boiler, Energy & Fuels, 25, 4952–60.

Patronelli S., Antonelli M., Tognotti L., Galletti C., 2018, Combustion of Wood-Chips in a Small-Scale Fixed-Bed Boiler: Validation of the Numerical Model through in-Flame Measurements, Fuel, 221, 128–37.

Rajh B., Yin C., Samec N., Hriberšek M., Kokalj F., Zadravec, M., 2018, Advanced CFD Modelling of Air and Recycled Flue Gas Staging in a Waste Wood-Fired Grate Boiler for Higher Combustion Efficiency and Greater Environmental Benefits, Journal of Environmental Management, 218, 200–208.

Schulte S., Heinzle J., Groß B., 2020, Reduction of Particulate Matter Emissions from a Pellet Boiler Using Primary Measures, Chemical Engineering & Technology, 43, 1506–13.